Polym. Bull. (2011) 67:1823–1836
DOI 10.1007/s00289-011-0511-2

ORIGINAL PAPER

Poly(sodium 4-styrene sulfonate) and poly(2-acrylamidoglycolic acid) nanocomposite hydrogels: montmorillonite effect on water absorption, thermal, and rheological properties

Bruno Urbano · Bernabé L. Rivas

Received: 6 February 2011 / Revised: 24 April 2011 / Accepted: 19 May 2011 /
Published online: 27 May 2011

Abstract A systematic study of water absorbency, thermal, and rheological properties was performed on nanocomposite hydrogels of poly(sodium 4-styrene sulfonate) (PSSNa) and poly(2-acrylamide glycolic acid) (PAAG). Montmorillonite was used as clay filler and was previously modified to hydrogel synthesis by addition of (3-acrylamide propyl)trimethylammonium chloride. Syntheses were carried out by in situ radical polymerization, using *N*,*N*-methylen-bis-acrylamide as crosslinker reagent. Nanocomposites showed an exfoliated morphology, confirmed by transmission electron microscopy and X-ray diffraction. The water absorption capacity (WAC) of unloaded PSSNa hydrogel was three times higher than for PAAG; due to clay addition, absorption capacity increased for PSSNa nanocomposites and decreased for PAAG. Finally, rheological properties of nanocomposite hydrogels were studied by both dynamic oscillatory test and shear creep analysis. Results showed improvements on mechanical properties, such as yield point, elastic recovery, and storage modulus as consequence of montmorillonite addition.

Keywords Nanocomposite · Hydrogel · Nanoclay · Rheology · X-ray diffraction

Introduction

In the last two decades, a significant interest in polymer–clay nanocomposites has developed, due to important changes in properties of polymers loaded with clays compared with unloaded polymers. The most important improvements include mechanical properties [1], flammability resistance [2], and barrier properties [3], among others, achieved using low clay content (3–7 wt%) [4].

B. Urbano · B. L. Rivas (✉)
Department of Polymer, Faculty of Chemistry, University of Concepción,
Casilla 160-C, Concepción, Chile
e-mail: brivas@udec.cl

In the field of nanocomposites an important advance is related with the synthesis of nanocomposite hydrogels. These materials consist in a tridimensional polymeric network, with hydrophilic functional groups and where clay layers are distributed and occluded inside a polymeric matrix in nano level [5]. Hydrogels have many applications: superabsorbents [6], drug delivery [7], membranes [8], sensors [9], etc.

Water absorption capacity, is one of the most important properties of these materials and it is closely related with crosslinking degree, where it is an inverse relationship. Thus, a hydrogel with low crosslinking degree allows high water absorption, although mechanical stability will be decreased in a swollen hydrogel. In hydrogel applications, a good performance in mechanical properties is necessary.

There are three synthesis methods for polymer–clay nanocomposites: intercalation from solution, in situ polymerization, and melt intercalation. Nevertheless, radical polymerization of a monomer, crosslinker, and initiator mixture is the frequent hydrogel synthesis procedure, and only in situ intercalative polymerization procedure can be used to hydrogel nanocomposites synthesis. In most common polymer–clay nanocomposites (based in polyolefin for example), the clay must be modified with quaternary ammonium surfactants in order to improve the interaction between hydrophobic and host polymeric matrix, thus favoring the intercalation of polymeric chains inside clay galleries. In the case of hydrogels, or hydrophilic polymeric matrix, some authors have reported the use of (2-acryloxyethyl)trimethylammonium chloride [10] and (3-acrylamidopropyl)trimethylammonium chloride [11] as intercalating agent. These compounds produce two effects. First, the quaternary ammonium cation interacts with the clay layer and replaces the hydrated cations by ion exchange process, producing an increase of interlayer distance to favor polymeric chains intercalation. Second, molecules bear a polymerizable double bond able to take part in polymerization reactions, thus favoring the delamination process in order to obtain an exfoliated morphology. It is worth noting that natural clays contain hydrated divalent counter ions (M^{+2}-MMT) to counteract the negative charges of clay layers, such as the montmorillonite K10. The presence of divalent ions causes an effect called "pillaring", decreasing clay expansion in solutions. Thus, natural MMT should be converted to sodium form (Na^{+}-MMT), before modification, to favor intercalation process [12].

Different clays have been used in hydrogel nanocomposites synthesis, like vermiculite [13], montmorillonite [14], attapulgite [15], etc. producing interesting changes, with respect to the unloaded hydrogel, in properties such as: swelling capacity [16], thermal, and mechanical stability [17], etc.

Rheological properties of nanocomposite hydrogels can be studied with the shear dynamic oscillatory test. A sinusoidal shear stress is applied and the out-of-phase (δ) strain response is measured. In the case of ideal solid and an ideal viscous liquid, this phase varies from 0° to 90°, respectively. In case of viscoelastic materials, the phase shift varies between 0° and 90°. The complex modulus (G^*) includes the contribution of both elastic and viscous response, and is given by following equation:

$$G^* = G' + iG'' \tag{1}$$

where G' corresponds to the storage modulus, which is a measurement of storage energy by elasticity and G'' is the loss modulus and is related with loss or dissipated

energy as consequence of viscosity. For hydrogels, an inverse relationship between G' and swelling capacity is expected; however, clay addition produces an increase of both storage modulus and swelling capacity. Additionally, G'' and G' can be related by loss factor or loss tangent defined by $\tan \delta = G''/G'$ and is an unidimensional measurement of energy dissipation [18].

The aim of this study is to study the montmorillonite effect on properties of hydrogel nanocomposites based in two monomers, sodium 4-styrene sulfonate and 2-acrylamide glycolic acid. Thermal properties of synthesized hydrogels were studied by differential scanning calorimetry (DSC) and thermogravimetric analysis (TGA), while rheological properties were studied by dynamic oscillatory and shear creep tests.

Experimental

Materials

The monomers 4-styrene sulfonic acid sodium salt hydrate (SSNa, Aldrich) and 2-acrylamide glycolic acid (AAG, Aldrich, 96%), and (3-acrylamidopropyl) trimethylammonium chloride (APTMA, Aldrich, 75 wt% in H_2O) as intercalating agent were used as received. *N*,*N*-methylene-bis-acrylamide (Aldrich, 99%) and ammonium persulfate (Aldrich, 98%) were used as crosslinker and initiator reagents, respectively. As clay filler, two kinds of montmorillonites (MMT) were used, theoretical formula $M_y^+(Al_{2-y}Mg_y)(Si_4)O_{10}(OH)_2{*}nH_2O$, Montmorillonite K10 (CEC 70–120 meq/100 g, Aldrich) and hydrophilic Bentonite higher than 99% of montmorillonite Nanomer® PGV (CEC 140 meq/100 g, Aldrich).

Montmorillonite modification

In order to prepare Na^+-MMT, 6.0 g of M^{2+}-MMT were added into 250 mL of an aqueous solution of 1 M sodium chloride. Mixture was stirred overnight, filtered, washed, and dried in an oven. Organophilic montmorillonite (OMMT) was prepared by adding 5.0 g of Na^+-MMT and 3 mL of (3-acrylamide propyl)trimethylammonium chloride to 200 mL of water, and the mixture was stirred for 24 h at 30 °C. Modified montmorillonite was filtered, then washed with an excess of distilled water until no chloride ion detection by $AgNO_3$ solution, and finally dried in a vacuum oven at 40 °C.

In situ polymerization

The hydrogel nanocomposites were synthesized by the radical in situ polymerization procedure (Scheme 1). Two different nanocomposites were synthesized: sodium 4-styrene sulfonate based hydrogel was polymerized using montmorillonite K10 and 2-acrylamide glycolic acid with Nanomer® PVG. Sodium 4-styrene sulfonate monomer (0.024 mol, 5.00 g) was added to a polymerization tube and 2-acrylamide glycolic acid monomer (0.030 mol, 5.00 g) into a second tube.

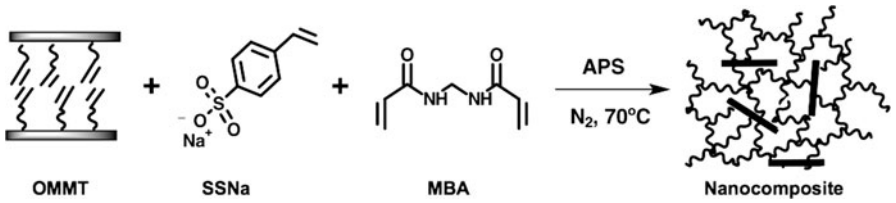

Scheme 1 Synthesis of hydrogel nanocomposite PSSNa

Organophilic montmorillonite was added in variable amounts (2.5–5.0 and 7.0 wt%, respect to monomer).

Additionally, a hydrogel without montmorillonite was synthesized in order to compare with nanocomposite hydrogels. Reagents *N*,*N*-methylen-bis-acrylamide (4 mol%) and ammonium persulfate (2 mol%) were used as crosslinker and initiator, respectively. The mixture was polymerized in a thermoregulated bath at 70 °C, under nitrogen atmosphere for 4 h. After the gel point was reached, hydrogels were extracted from reactor, washed several times with distilled water and dried in a vacuum oven until constant weight. Grinded hydrogels with a particle size range of 250–180 μm, were used for all experiments.

Characterization

Nanocomposite hydrogel functional groups were evaluated by infrared spectroscopy, analyses were carried out in a Perkin Elmer 1760-X spectrometer with Fourier transform, in a range of 4,000–400 cm^{-1}, using KBr pellets. In order to determine montmorillonite interlayer distances and its change from pristine MMT, organophilic MMT and montmorillonite dispersed within nanocomposites, X-ray diffraction (XRD) analysis were carried out and the analyses were performed in an RIGAKU instrument, Geigerflex model diffractometer (CuKα tube, 40 kV, 20 mA) in a range of 2° to 15° 2θ at 1°/min. Diffraction results were complemented with transmission electron microscopy (TEM), in the JEOL/JEM 1200 EX II instrument.

The nanocomposite thermal properties were studied in a DSC instrument Q20 TA Instrument, heating rate 10 °C/min, using dry nitrogen at flow rate 40 mL/min. Additionally, thermogravimetric analysis (TGA) were performed in a Perkin Elmer Model 7 instrument, in a range 0–550 °C and heating rate of 10 °C min^{-1}.

The ability of nanocomposites to swell in aqueous solution was determined by the water absorption capacity (WAC). A known amount of resins (0.05 g) were contacted with 80 mL of distilled water at pH 5 for 48 h. Once equilibrium absorption was reached, the mass of the swollen resins was determined. The WAC value was determined by

$$\mathrm{WAC} = \frac{w_s - w_d}{w_d} \tag{2}$$

where w_s and w_d correspond to mass of swollen and dry resin, respectively. Finally, using the swollen resins, rheological properties were determined by a parallel plate rheometer Haake Rheostress 1, gap 1 mm, at 25 °C and under control stress mode.

Storage (G') and loss (G'') modulus were determined as function of applied stress and frequency by oscillatory sweeps. Additionally, shear creep and recovery analysis were performed in order to determine properties such as compliance and elastic recovery.

Results and discussion

Infrared spectroscopy

FTIR spectra of organophilic and Na^+-MMT are shown in Fig. 1. Montmorillonite spectrum presents its characteristic vibration bands at 3643 cm^{-1} (O–H st), 3347 cm^{-1} (H_2O st), and 1034 cm^{-1} (Si–O st). In the case of modified montmorillonite, the spectrum presents both MMT and (3-acrylamido propyl)trimethylammonium chloride characteristic bands at 3046 cm^{-1} (C = C st), 1670 cm^{-1} (C=O st), and 1490 cm^{-1} (N^+-H st). Figure 1 also shows hydrogel PSSNa and PAAG FTIR spectra. PSSNa presents bands at 2926 cm^{-1} (C–C st), 1644 cm^{-1} (C=C), 1188 cm^{-1} (C–H, 1,4 substitution), and 1042 cm^{-1} (S=O st), in case of PAAG 1748 cm^{-1} (C=O st), 1661 cm^{-1} (C–N st), 1533 cm^{-1} (COO as st), 1218 cm^{-1} (C–O st, acid), and 1089 cm^{-1} (C–O st, alcohol). Montmorillonite band associated to Si–O st does not appear clearly in the nanocomposites' spectra due to a small amount of loading.

It is also important to indicate that the vibration band associated with lateral hydroxyl groups of the clay platelet (3,632 cm^{-1}) [19], which is present at MMT and OMMT spectra, disappears in nanocomposites, suggesting a covalent interaction between clay platelet and polymeric matrix with edge hydroxyl groups [20].

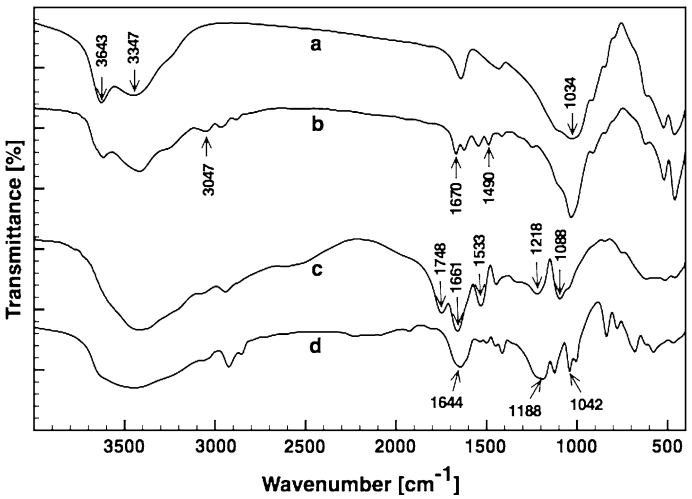

Fig. 1 FTIR spectra of (*a*) MMTK10, (*b*) OMMT, (*c*) PAAG-5% O-Nanomer®, and (*d*) PSSNa-5% OMMT

X-ray diffraction

Figure 2 shows X-ray patterns of both classes of montmorillonite used. Interlayer distances were determined for Na^+-MMT, OMMT, and OMMT in hydrogels. Diffractograms of Na^+-MMT have a peak corresponding to d_{001} plane; in agreement with Bragg's law, the peak is placed around 8.3° 2θ corresponding to a distance of 1.04 nm and 6.2° 2θ corresponding to 1.30 nm for MMTK10 and Nanomer®, respectively.

After modification with (3-acrylamide propyl)trimethylammonium chloride, both pattern peaks were displaced towards lower angles, indicating that the interlayer distance increased as consequence of intercalation process. However, the MMTK10 pattern also shows the same peak of Na^+-MMT, suggesting that intercalation was not completed. Additionally, peaks of modified montmorillonite showed a width increase, indicating a loss of regularity of interlayer distances in stacked layers as consequence of different degrees of intercalation.

With respect to the distribution of APTMA molecules in the interlayer region, XRD [1] and FTIR [21] studies have proposed several alkyl aggregation models. Models were proposed using surfactant of variable alkyl chain length (C_6–C_{18}); in the case of the shortest alkyl chain surfactant used (C_6), the models indicate that chains can be arranged in lateral monolayers and/or paraffin-type monolayers. In the case of the studied OMMT, the change in the interlayer distance observed in diffractogram was 6.7 and 5.02 Å for Nanomer® and MMTK10, respectively. The intercalating agent has an approximate length of 7.5 Å (similar to C_6 surfactant), and thus, suggesting that the (3-acrylamide propyl)trimethylammonium chloride molecule aggregation is a paraffin-type or lateral monolayer structure.

Finally, in the diffractograms of OMMT within nanocomposites, no peak diffraction appears in the pattern, neither MMTK10 nor Nanomer, indicating that the clay layers are well separated from each other and individually dispersed in the continuous polymer matrix. As a result, the X-ray beam does not diffract, and thus an exfoliate morphology is suggested. The exfoliation process could be produced, considering that the double bond ruptures within interlayer region during the polymerization process, and thus the released energy and growing chain tension favored layers delamination of clay layers.

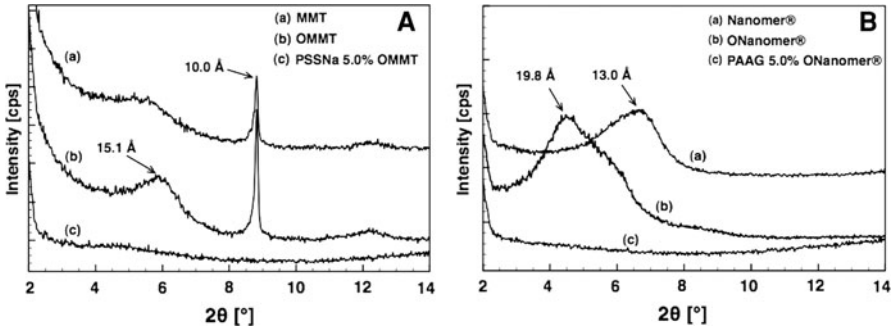

Fig. 2 XRD patterns of **a** MMTK10 and **b** Nanomer® PGV

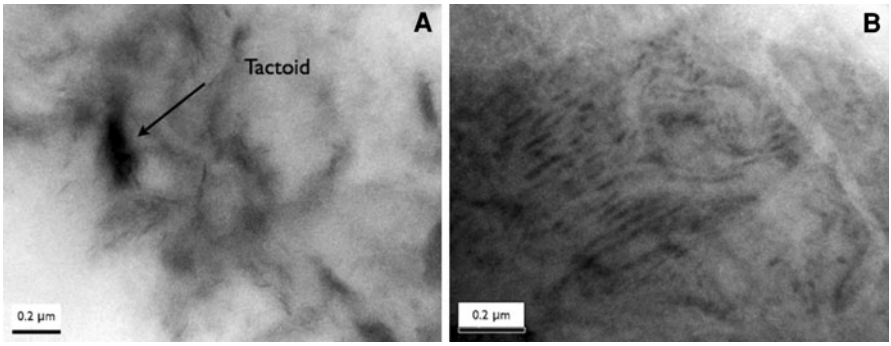

Fig. 3 TEM micrographs of **a** PAAG-5% O-Nanomer® and **b** PSSNA-5% OMMT

Transmission electron microscopy

Transmission electron microscopy (TEM) was performed in order to complement the XRD results. TEM gives visual and direct information about clays, morphology, and spatial distribution in a local area of sample. Figure 3 shows the micrographs of nanocomposites loaded with 5% for PSSNa and PAAG clearly indicates the presence of clays in the hydrogels. With respect to clay distribution, in the micrograph of PAAG 5%, a single clay layer can be observed, suggesting exfoliate morphology; however, an agglomeration of clay layers, called "tactoid", is also observed in the same micrograph, indicating that no exfoliation occurs. In the PSSNa 5% micrograph, a clay layer with a regularity distribution suggesting intercalated morphology is also observed. Considering that the TEM technique provides reduced local information and diffractogram peaks correspond to a mean of diffracted beams, it is concluded that the nanocomposites possess an exfoliate morphology.

Thermal properties

Nanocomposite thermal properties were studied by differential scanning calorimetry (DSC) and thermogravimetric analysis (TGA). Table 1 summarizes specific data of the nanocomposite thermal study. The PSSNa nanocomposites presented differences in glass transition temperatures (T_g) with respect to unloaded hydrogel: specifically hydrogels PSSNa-2.5% and 7.0% possess a T_g approximately 15 °C higher than unloaded PSSNa, while PSSNa-5.0% presented only a slight increase. These results can be explained as due to the loss in rotational and translational chain movements resulting from the confinement of polymeric chains within clay galleries [22]. In contrast, a decrease of T_g was observed for the PAAG hydrogel with 2.5 and 5.0% loading. A decrease of glass transition temperature is an unexpected result, considering the argument of nano-confinement of polymeric chains; however, similar tendencies have been reported. It is worth mentioning that there is no general agreement about the change of T_g in polymer–clay nanocomposites: some reports show an increase of T_g, others a decrease, and other reports report no effect of clay

Table 1 Thermal behavior and T_g of nanocomposite resins, measured under N_2 atmosphere and heating rate of 10 °C min^{-1}

Sample acronym	1st T_{deg} (°C)[a]	Weight loss (%)[b]				T_g (°C)
		200 °C	300 °C	400 °C	500 °C	
PSSNa-0%OMMTK10	445.2	1.3	2.5	3.7	12.8	69.5
PSSNa-2.5%OMMTK10	444.7	0.7	1.7	3.1	13.9	86.0
PSSNa-5.0%OMMTK10	460.3	0.6	1.1	2.5	12.2	69.9
PSSNa-7.0%OMMTK10	448.5	0.6	1.5	3.0	12.5	85.0
PAAG-0% O-Nanomer®	214.2	24.1	81.7	85.4	89.6	70.8
PAAG-2.5% O-Nanomer®	196.0	44.1	68.7	76.1	85.7	57.9
PAAG-5.0% O-Nanomer®	211.0	35.2	71.6	78.9	86.2	55.6
PAAG-7.0% O-Nanomer®	194.3	34.2	56.1	66.7	79.8	72.3

[a] Value obtained from 1st derivate of weight loss respect to temperature (d%/dT)

[b] Weight loss percentages were calculated by the difference of percentage at 150 °C and the percentage at indicated temperature. The weight loss at 150 °C was used in order to discard crystallization water

nano-confinement on glass transition [23–25]. Further studies are needed to define the effective change of T_g.

Table 1 also shows the first degradation temperature of hydrogel nanocomposites and the weight loss percentage at different temperatures. All the PSSNa hydrogels present essentially the same degradation temperature (445 °C); except for PSSNa-5.0% with a degradation temperature approximately 15 °C higher respect other than the hydrogels. In case of PAAG, degradation temperatures of PAAG-2.5% and 7.0% are approximately 15 °C lower than those nanocomposites without montmorillonite. It is important to mention that onset decomposition temperatures of nanocomposites are higher than that unloaded hydrogel, both PAAG and PSSNa hydrogels (not showed). This may be attributed to the better interaction between clay layers and polymeric network. The weight loss mainly decrease when clay are present in nanocomposites, and in the range of 300 and 400 °C all nanocomposites lost less weight compared with unloaded hydrogels. The hydrogels PSSNa-5.0% and PAAG-7.0% presents the lowest loss. Between 300 and 500 °C, PAAG-2.5% and 5.0% present similar weight loss values, possibly due to a low clay loading during the synthesis.

Water absorption capacity

Figure 4 shows nanocomposite water absorption capacity (WAC) for different clay loadings. Nanocomposites with sulfonate groups show good water absorbency (146.0 g H_2O/g nanocomposite hydrogel) because sulfonate groups act as strong acid and are totally ionized in a whole pH range; they have the ability able to produce of major solvation spheres and improved water absorption [26]. Respect to observed tendencies as a function of clay content, PSSNa hydrogels show an increase of WAC with clay addition, reaching a maximum at 178.0 g H_2O/g nanocomposite hydrogel for PSSNa-2.5%, after WAC decreases until similar values

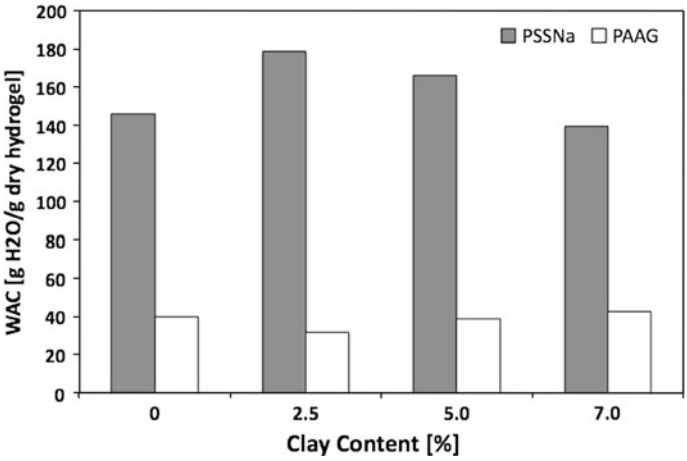

Fig. 4 Hydrogel water absorption capacity (WAC) as function of clay content

of unloaded hydrogel. The increase of WAC can be explained due to hydrophilicity added by clay dispersion within nanocomposites and also to the improved elastic properties (explained below at rheological results). Briefly, results obtained by shear creep test show that nanocomposite loaded with 2.5%, improved the elastic performance allowing a major expansion of polymeric network, and thus hydrogel swell it more compared with unloaded hydrogel. In case of PSSNa-5.0% and 7.0%, WAC values decrease, 166 and 139 gH_2O/g for nanocomposite hydrogel, respectively. These values are in agreement with the rheological results (shear creep), where hydrogels presented a lower elastic performance than that PSSNa 2.5% (see Table 2) and show a similar behavior to unloaded resins.

In comparison with PSSNa hydrogels, nanocomposite resins based in 2-acrylamide glycolic acid groups present a decrease on WAC (39.8 g H_2O/g nanocomposite resin), and an opposite behavior with clay addition. Observed differences can be explained by considering functional groups properties in aqueous solution. For resins based in 2-acrylamide glycolic groups, swelling is less favored due to low ionization: carboxylate groups are partially ionized and nitrogen atoms partially protonated at pH 5 [27], and thus these groups cannot contribute to osmotic pressure. Additionally, hydrogen bond interaction can occur between carboxylic acid groups with hydroxyl and oxygen atoms in clays layers [28]. Also, nitrogen atoms are partially protonated at pH 5 and these groups can interact with clay surface by ion exchange, similar to APTMA molecules behavior. As a result, the hydrophilicity of the polymeric matrix is reduced and therefore water absorption decreases.

As was explained in the infrared spectroscopy section, the lack of a vibration band in the hydrogel's IR spectrum, related with the hydroxyl edge of clay layers, suggests a covalent interaction with polymeric matrix [20].

Increasing the clay content, WAC also increases until obtaining values similar to that of unloaded resins. This behavior can be explained considering that the clay layer tends to aggregate, increasing the sizes [29] and reducing the surface layer

Table 2 Shear creep-recovery analysis for PSSNa and PAAG nanocomposites as function of clay loading

Quantity	PSSNa-0% MMTK10	PSSNa-2.5% MMTK10	PSSNa-5% MMTK10	PSSNa-7% MMTK10
γ-r/γ-max [%]	41.1	88.7	47.6	38.8
$Je_0 \times 10^{-3}$ (Pa^{-1})	3.0	1.1	4.1	2.5
G (Pa)	326.9	909.4	238.5	397.7
Quantity	PAAG-0% Nanomer®	PAAG-2.5% Nanomer®	PAAG-5% Nanomer®	PAAG-7% Nanomer®
γ-r/γ-max [%]	76.2	90.6	72.2	76.1
$J_{e0} \times 10^{-4}$ (Pa^{-1})	6.1	2.1	5.9	5.2
G (Pa)	1,640	4,717	2,526	1,898

interaction with polymeric matrix, and thus functional groups are able to contribute to osmotic pressure.

Rheology

Shear creep analysis

In a creep-recovery experiment, a constant shear stress (σ_0) is applied for a period of time. In a viscoelastic material, the ratio between deformation respect time and stress ($\gamma_{(t)}/\sigma_0$) is called compliance (J), which is a measurement of deformation per unit of applied stress. When the compliance shows a linear dependence with respect to time in the creep region and extrapolation of compliance to zero (t_0) is considered, and then compliance is called steady-state compliance (J_{e0}). Table 2 shows results obtained by shear creep analysis as function of clay loading.

It is observed that resins loaded with 2.5% of montmorillonite, both PSSNa and PAAG nanocomposites, present a lower steady-state compliance and a higher modulus, defined as inverse of compliance ($J = G^{-1}$), with respect to unloaded resin and the rest of nanocomposites. This result clearly indicates that resins have major resistance to deformation at t_0 as a consequence of clay addition. Moreover, the elastic recovery ratio (defined as recovery deformation (γ_r) divided by maximum deformation (γ_{max}) of material) presents significant changes for resins with 2.5% of montmorillonite. From PSSNa-0% to PSSNa-2.5%, the elastic recovery is duplicated, demonstrating the clear effect of clays over hydrogel rheological properties. Additionally, with increasing clay content, the elastic recovery presents drops similar to the swelling capacity. On other hand, for PAAG-7.0% and 5.0%, the elastic recovery values were similar to the values of unloaded hydrogel; however, PAAG-2.5% presents an increase of 15% with respect to the unloaded PAAG hydrogel. These results clearly show the montmorillonite effect on hydrogel mechanical properties, and specifically on elasticity.

Oscillatory dynamic analysis

In addition to the creep study, resins were analyzed by the oscillatory dynamic test. Figure 5 shows curves of storage modulus, for PSSNa and PAAG nanocomposites with different clay loading, as function of applied stress at 1 Hz of frequency and angular frequency at 1 Pa of stress. In graph A, the linear viscoelastic region (LVR) is observed where resins storage (G') and loss (G'') modulus are independent of applied stress and in this region $G' > G''$, which indicates that the material has a gel character. On other hand, the stress where LVR ends and the G' drop begins is called yield point and corresponds to the beginning of plastic deformation. The fact that this point is located in the LVR indicates is a reversible viscoelastic condition. It is clear that the PSSNa 2.5% has a yield point higher than other resins, indicating that these resins resist greater stress before deformation. A similar behavior was found for the flow point, where viscoelasticity is irreversible, which corresponds to crossover point between G'' and G' where $G'' > G'$ (inserted plot in A). In the case of PAAG hydrogels, a crossover was found for only some nanocomposites, and G' was maintained higher than G''.

In case of G' as a function of angular frequency, nanocomposite curves present differences in the angular frequency range study (0.1 and 100 rad·s^{-1}). In plot B, the storage modulus of PSSNa-2.5% is observed to present less variation or "flatness" as a function of frequency; the highest variation was found for

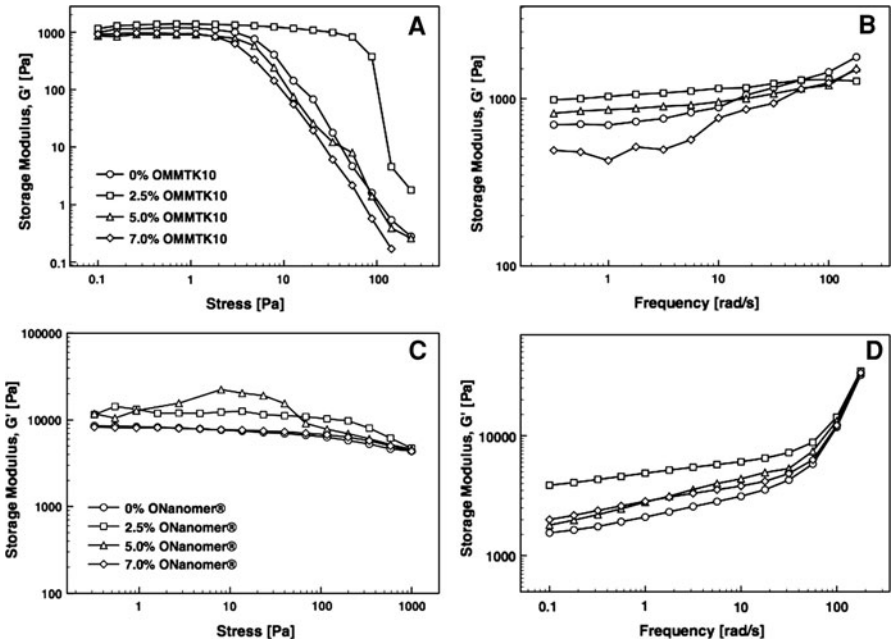

Fig. 5 Storage modulus (G') as function of applied stress and angular frequency for different clay loadings. Graph **a** and **b** correspond to PSSNa hydrogel, and **c** and **d** to PAAG hydrogels

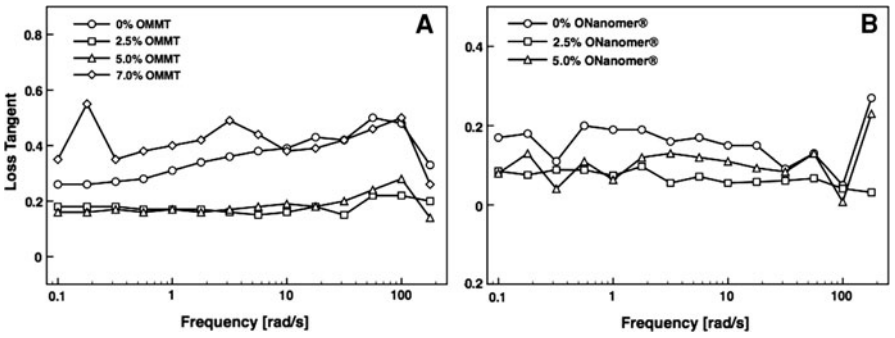

Fig. 6 Loss tangent graphs for **a** PAAG and **b** PSSNa

PSSNa-0%. These results prove that montmorillonite gives an additional stability to hydrogel.

In case of PAAG hydrogels (plot D), no significant variations were found compared to PSSNa hydrogels. The range of stress applied did not present a yield point, however, storage modulus for PAAG 2.5% is higher than other resin. As a function of frequency, the storage modulus is observed to increase rapidly at higher angle frequencies. This result can be explained by considering the relaxation time of hydrogel because stressed polymeric chains at higher frequencies do not have the enough time to relax and the instrument measures a more solid-like character.

From the G' and G'' values, it is possible to obtain the loss tangent ($\tan \delta = G''/G'$) and represent the ratio between dissipated and storage energy. The loss tangent varies between $0 < \tan \delta < \infty$, where $\tan \delta = 0$ is an ideal solid behavior (elastic) and $\tan \delta = \infty$ corresponds to ideal viscous material. In the case of gels, it is accepted that $\tan \delta < 1$ (where $G' > G''$) [30]; for weak gels, $\tan \delta > 0.1$ [31]. Considering the previously mentioned results, Fig. 6 shows the loss tangent results for nanocomposites with different clay loadings with respect to the angular frequency applied; $\tan \delta$ values are observed to be constant in the entire range of frequencies applied and its oscillation is between 0–0.2 and 0.1–0.4 for PAAG and PSSNa hydrogels, respectively, indicating that both kinds of hydrogel have a gel character and relatively stronger character for PAAG hydrogel.

Conclusions

Synthesized nanocomposite hydrogels showed significant changes in swelling and rheological properties due to montmorillonite addition. X-ray diffraction indicated that nanocomposites have an exfoliated structure, which was confirmed by transmission electron microscopy. Water absorption capacity presented opposite behavior with clay addition: while PSSNa increased WAC, PAAG decreased. Hydrogel thermal properties only slightly changes in weight loss between loaded and unloaded nanocomposites. Rheological analysis showed important changes in nanocomposites mechanical properties. It was demonstrated that PSSNa and PAAG hydrogels loaded with 2.5% of montmorillonite presented better deformation

resistance, stability for different stress frequencies, diminished compliance and better elastic recovery with respect to unloaded hydrogel and the rest of synthesized nanocomposites.

Acknowledgments The authors thank to FONDECYT (Grant No 1070542), PIA (Grant Anillo ACT 130), and "Centro de Investigación de Polímeros Avanzados" (CIPA-Chile) the financial support. B. Urbano, acknowledges to ''Comisión Nacional de Investigación Científica y Tecnológica'' (CONICYT-Chile) for funds received.

References

1. Alexandre M, Dubois P (2000) Polymer-layered silicate nanocomposites: preparation, properties and uses of a new class of materials. Mater Sci Eng 28:1–63
2. Qin H, Zhang S, Zhao C, Hu G, Yang M (2005) Flame retardant mechanism of polymer/clay nanocomposites based on polypropylene. Polymer 46:8386–8395
3. Meneghetti P, Qutubuddin S (2006) Synthesis, thermal properties and applications of polymer–clay nanocomposites. Thermochim Acta 442:74–77
4. Pavlidou S, Papaspyrides CD (2008) A review on polymer-layered silicate nanocomposites. Prog Polym Sci 33:1119–1198
5. Schexnailder P, Schmidt G (2009) Nanocomposite polymer hydrogels. Colloid Polym Sci 287:1–11
6. Kabiri K, Omidian H, Hashemi SA, Zohuriaan-Mehr MJ (2003) Synthesis of fast-swelling superabsorbent hydrogels: effect of crosslinker type and concentration on porosity and absorption rate. Eur Polym J 39:1341–1348
7. Chen J, Park K (2000) Synthesis and characterization of superporous hydrogel composites. J Control Release 65:73–82
8. Gudeman LF, Peppas NA (1995) pH-Sensitive membranes from poly (vinyl alcohol)/poly (acrylic acid) interpenetrating networks. J Membr Sci 107:239–248
9. Richter A, Paschew G, Klatt S, Lienig J, Arndt K-F, Adler H-JP (2008) Review on hydrogel-based pH sensors and microsensors. Sensors 8:561–581
10. Kellera L, Decker C, Zahouily K, Benfarhi S, Meins JML, Miehe-Brendle J (2004) Synthesis of polymer nanocomposites by UV-curing of organoclay–acrylic resins. Polymer 45:7437–7447
11. Lee W-F, Chen Y-C (2005) Effect of intercalated reactive mica on water absorbency for poly(sodium acrylate) composite superabsorbents. Eur Polym J 41:1605–1612
12. Chou C-C, Chiang M-L, Lin J-J (2005) Unusual intercalation of cationic smectite clays with detergent-ranged carboxylic ions. Macromol Rapid Commun 26:1814–1845
13. Zheng Y, Li P, Zhang J, Wang A (2007) Study on superabsorbent composite XVI. Synthesis, characterization and swelling behaviors of poly(sodium acrylate)/vermiculite superabsorbent composites. Eur Polym J 43:1691–1698
14. Lee W-F, Yang L-G (2004) Superabsorbent polymeric materials. XII. Effect of montmorillonite on water absorbency for poly(sodium acrylate) and montmorillonite nanocomposite superabsorbents. J Appl Polym Sci 92:3422–3429
15. Zhang J, Wang A (2007) Study on superabsorbent composites. IX: Synthesis, characterization and swelling behaviors of polyacrylamide/clay composites based on various clays. React Funct Polym 67:737–745
16. Paranhos CM, Soares BG, Oliveira RN, Pessan LA (2007) Poly(vinyl alcohol)/clay-based nanocomposite hydrogels: swelling behavior and characterization. Macromol Mater Eng 292:620–626
17. Tanaka Y, Gong JP, Osada Y (2005) Novel hydrogels with excellent mechanical performance. Prog Polym Sci 30:1–9
18. Krevelen DWV, Nijenhuis KT (2009) Properties of polymers, 4th edn. Elsevier BV, Amsterdam
19. Bukka K, Miller JD (1992) FTIR study of deuterated montmorillonites: structural features relevant to pillared clay stability. Clays Clay Miner 40:92–102
20. Wu J, Lin J, Li G, Wei C (2001) Influence of the COOH and COONa groups and crosslink density of poly(acrylic acid)/montmorillonite superabsorbent composite on water absorbency. Polym Int 50:1050–1053

21. Vaia RA, Teukolsky RK, Giannelis EP (1994) Interlayer structure and molecular environment of alkylammonium layered silicates. Chem Mater 6:1017–1022
22. Leszczynska A, Pielichowski K (2008) Application of thermal analysis methods for characterization of polymer/montmorillonite nanocomposites. J Therm Anal Calorim 93:677–687
23. Huang J-C, Zhu Z-k, Yin J, Qian X-f, Sun Y-Y (2001) Poly(etherimide)/montmorillonite nanocomposites prepared by melt intercalation: morphology, solvent resistance properties and thermal properties. Polymer 42:873–877
24. Li Y, Ishida H (2005) A study of morphology and intercalation kinetics of polystyrene-organoclay nanocomposites. Macromolecules 38:6513–6519
25. Liu X, Wu Q (2001) PP/clay nanocomposites prepared by grafting-melt intercalation. Polymer 42:10013–10019
26. Zagorodni AA (2007) Ion exchange materials properties and applications, 1st edn. Elsevier BV, Amsterdam
27. Rivas BL, Quilodrán B, Quiroz E (2003) Removal properties of crosslinked poly(2-acrylamido glycolic acid) for trace heavy metal ions: effect of ph, temperature, contact time, and salinity on the adsorption behavior. J Appl Polym Sci 88:2614–2621
28. Tran NH, Dennis GR, Milev AS, Kannangara GSK, Wilson MA, Lamb RN (2005) Interactions of sodium montmorillonite with poly(acrylic acid). J Colloid Interface Sci 290:392–396
29. Xia X, Yih J, D'Souza NA, Hu Z (2003) Swelling and mechanical behavior of poly(N-isopropylacrylamide)/Na-montmorillonite layered silicates composite gels. Polymer 44:3389
30. Mezger TG (2006) The rheology handbook: for users of rotational and oscillatory rheometers, 2nd edn. Vincentz Network GmbH & Co., Hannover
31. Can V, Abdurrahmanoglu S, Okay O (2007) Unusual swelling behavior of polymer–clay nanocomposite hydrogels. Polymer 48:5016–5023